



OTC 17736

## Hindcast Study of Winds, Waves and Currents in Northern Gulf of Mexico in Hurricane Ivan (2004)

Andrew T. Cox and Vincent J. Cardone, Oceanweather Inc; Francois Counillon, Nansen Environmental and Remote Sensing Center; David Szabo, Ocean Numerics

Copyright 2005, Offshore Technology Conference

This paper was prepared for presentation at the Offshore Technology Conference held in Houston, Texas, U.S.A., 2-5 May 2005.

This paper was selected for presentation by an OTC Program Committee following review of information contained in an abstract submitted by the author(s). Contents of the paper, as presented, have not been reviewed by the Offshore Technology Conference and are subject to correction by the author(s). The material, as presented, does not necessarily reflect any position of the Offshore Technology Conference or its officers. Electronic reproduction, distribution, or storage of any part of this paper for commercial purposes without the written consent of the Offshore Technology Conference is prohibited. Permission to reproduce in print is restricted to an abstract of not more than 300 words; illustrations may not be copied. The abstract must contain conspicuous acknowledgment of where and by whom the paper was presented.

### Abstract

The time varying fields of surface winds, sea state and currents associated with Hurricane Ivan (2004) in the Northern Gulf of Mexico are specified through the implementation and application of advanced numerical wind, wave and ocean hindcast models, all adapted to the entire Gulf of Mexico at higher resolution than used in previous simulations of tropical cyclones in this basin. An extensive validation of the wind and wave hindcast indicates that the storm response is specified with 10% or better accuracy. No public domain current measurements were available in Ivan to validate the current model results but validation of the same modeling technology against the extensive currents measurements in previous Gulf of Mexico hurricanes suggests that the spatial and vertical structure of the primary current speed response to Ivan are reasonably well simulated.

### Introduction

The objective of this study is to develop a comprehensive, definitive and reliable database of wind, sea state and currents associated with Hurricane Ivan (2004) in the Northern Gulf of Mexico (GOM), through the implementation and application of advanced numerical wave and current hindcast models. The database is not only of intrinsic value, but also a critical element of investigations of the considerable impact of Ivan on GOM offshore operations and infrastructure. In this sense the study and objectives are analogous to those of our previous comprehensive studies of Hurricanes Andrew (1,2) and Lili (3). Like these past studies this hindcast builds upon methods that have continuously evolved over the past 35 years to measure, describe, understand and model the surface marine meteorological characteristics of GOM hurricanes and the corresponding ocean response to their passage (4,5,6,7). This methodology has been applied in major joint industry programs to hindcast all hurricanes affecting the Gulf of Mexico since 1900 and to develop reliable extreme event metocean design data (8,9,10).

Many of the hurricanes hindcast in government and industry sponsored studies cited above have included high quality wind, wave, water level and ocean current measurements

(Audrey, 1957; Bertha, 1957; Carla, 1961; Camille, 1969; Edith, 1971; Delia, 1973; Frederic, 1979; Danny, 1985; Juan 1985, Andrew, 1992, Georges, 1998, Lili, 1992). These validation studies (e.g.11,12) demonstrated the accuracy of our hindcast methods when applied to specify peak sea states (significant wave height) at an arbitrary site in a Gulf of Mexico hurricane (bias of less than 0.5 m, mean absolute error of less than 1.0 m and scatter index of 10-15%). The inner core of Ivan passed over NOAA data buoy 42040 and other nearby buoys experienced severe winds and sea states thereby providing measurements of the profile of surface winds and sea state across the storm that are invaluable in the validation of the hindcast reported here.

The ocean current model used is the state-of-art Hybrid Coordinate Ocean Model (HYCOM) (13) which has already been proven to be superior to other models for the combined modeling of the deep ocean and the continental shelf, providing a consistent bridging between these dynamically very different regimes. No public domain current measurements were acquired in Ivan making reliance on accurate current modeling even more critical.

### Specification of the Wind Field

**Storm History.** The detailed track of Ivan in the Northern Gulf of Mexico is shown in Figure 1 along with the locations of NDBC buoy stations. The center of Ivan passed about mid-way between the offshore buoys 42001 (Mid-Gulf buoy located at 25°55'12"N 89°40'48"W in 3,246 meters of water and 42003 (East-Gulf buoy located at 26 00 32 N 85 54 50 W in 3164 meters of water) and then very close to buoy 42040 (Mobile-South located at 29 12 88 12 in 444 meters of water). 42001 and 42003 are 10-meter discuss buoys with wind measurements at 10 meters above the sea surface while 42040 is a smaller 3-meter discuss which measures winds at 5 meters above the sea surface. The center of the storm also passed near 42007 (Biloxi buoy located at 30 06 N, 88 48 W in 13.4 meters of water) thereby providing a fairly rare set of measurements close to shore and in very shallow water near a strong landfalling hurricane. 42007 is also a 3 m discuss type.

The most interesting set of buoy measurements are those made by 42040 but unfortunately a complete set of data was denied by the fact that the buoy broke loose from its mooring at the height of the storm and drifted southward over the ensuing days as shown in Figure 1. Based on the best track, the last few observations seemed to capture near peak conditions in the front side of Ivan's eyewall. The maximum recorded 10-minute average wind speed of 28.3 m/s (at 5 m) with associated wind direction of 54 degrees (from northeast) was recorded at 2250 UTC 9/15/04. A peak gust of 37.7 m/s was recorded at 2050 UTC 9/15/04. By the time of the last quality controlled observation, at 0000 UTC 9/16/04, wind speeds (10-minute average at 5 meters) had decreased to 26.5 m/s suggesting that the buoy was entering the northern part of the eye. These wind speeds are much lower than expected of a storm of Ivan's intensity and all other estimates of maximum surface winds (see below) and our hindcast suggest strongly that these wind speeds are biased quite low (even after allowing for anemometer height) probably by buoy motion, wave sheltering and other effects. At 0000 UTC 9/16/04 a maximum significant wave height of 15.96 m was estimated from the wave spectrum of the last quality controlled wave record, which is probably the record high sea state measurement for a NOAA data buoy. This peak is more than 2 meters greater than the peak significant recorded in Saffir Simpson Scale Category 5 Hurricane Camille (1969) at ODGP Station 1 in the right front quadrant of the eye wall. It is remarkable that Ivan, a category 3 storm as it approached the Gulf coast, was able to raise sea states thought to be associated only with Category 4 or 5 storms. Ivan also generated a very large area of severe sea states in the eastern GOM. The track passed about 90 NM west of 42003 where a peak HS of 11.7 m was measured, and passed about 120 NM east of 42001 where a peak HS of 8.8 m was measured. This extreme intensity and size of Ivan, therefore, posed an exceptional challenge to the hindcast methodology applied.

Ivan entered the Gulf of Mexico as a Category 5 hurricane near 0000 UTC 9/14/05 as its center passed just west of the extreme western tip of Cuba, with central pressure of 914 mb and peak sustained wind speed of 140 knots (sustained wind speed is the peak 1-minute average wind speed at 10-meters elevation over water). As Ivan moved northwestward in the Gulf it slowly weakened as its circulation encountered westerly tropospheric wind shear and, further north, cooler shelf waters; nevertheless, it did not weaken below Category 3 at 105 knots when it made landfall just west of Gulf Shores Alabama at approximately 0700 UTC 9/16/04. A number of independent data sources and types confirm this general level of intensity in the 12 hours before landfall including: 120 knot maximum aircraft flight level wind speeds which reduce to approximately 108 knots sustained surface wind using a standard reduction factor; coastal radar Doppler radar velocities of about 120 knots, which reduce to 104 knots using the appropriate reduction factor; measured sustained wind speeds of 102 knots with gust to 135 knots at an elevation of 400 feet on the Ram Powell (VK956) platform. The standard reduction factor from peak sustained 1-minute wind speed at 10-meter elevation to peak 30-minute average wind speed is 1.24. A peak sustained wind speed of 105 knots, therefore,

transforms to a peak average wind speed at 10-meter elevation of 85 knots or 43.6 m/s. Maximum storm surges measured by coastal gauges at Pensacola Bay, Florida and Orange Beach, Alabama were 2.95 meters (9.68 feet) and 2.80 meters (9.17 feet) respectively. The NOAA Tropical Prediction Center storm report for Ivan is available at <http://www.nhc.noaa.gov/2004ivan.shtml>.

**Data Collection.** The success of the ocean response modeling rests critically on the accuracy of the wind fields used to force the models. To achieve this accuracy we utilized a proven wind field hindcast methodology and assembled and processed all of the data needed for its optimum application. The pertinent data sets assembled for this study for wind field (and wave model) analysis and validation consist of:

1. Aircraft reconnaissance of Hurricane Ivan obtained from NOAA and U.S. Air Force hurricane hunter aircraft, including vortex messages as well as continuous flight level wind speed, direction, D-Value, air temperature.
2. Gridded and image fields of marine surface wind composites from the Hurricane Research Division HWnd analysis of Ivan
3. Synoptic observations from NOAA buoy and C-MAN stations
4. Synoptic observations from coastal and land stations obtained from the GTS (Global Transmission System) in real time
5. NOAA NHC/TPC advisories including intensity and position at 3-hourly intervals.
6. NHC/TPC best track data
7. NHC/TPC Tropical Storm Report
8. Composite NWS radar imagery
9. Loops of NOAA GOES visual, infrared and water vapor imagery
10. NWS synoptic weather analysis charts
11. NCEP model wind fields
12. QUIKSCAT scatterometer winds
13. TOPEX altimeter winds and waves
14. ERS-2 altimeter winds and waves
15. Report of surge heights from operational gauge networks
16. NWS storm information

**Wind Analysis Model.** The method used in this study has been applied in over three-dozen studies involving almost all basins on the globe within which tropical cyclones can occur. The method starts from raw data whenever possible and includes an intensive reanalysis of traditional cyclone parameters such as track and intensity (in terms of pressure) and then develops new estimates of the more difficult storm parameters, such as the shape of the radial pressure profile and the ambient pressure field within which the cyclone is embedded. The time histories of all of these parameters are specified within the entire period to be hindcast. Storm track and storm parameters are then used to drive a numerical primitive equation model of the cyclone boundary layer to generate a complete picture of the time-varying wind field associated with the cyclone circulation itself.

The model, first developed into a practical tool in the ODGP can provide a fairly complete description of time-space evolution of the surface winds in the boundary layer of a tropical cyclone from the simple model parameters available in historical storms. The model is an application of a theoretical model of the horizontal airflow in the boundary layer of a moving vortex. That model solves, by numerical integration, the vertically averaged equations of motion that govern a boundary layer subject to horizontal and vertical shear stresses. The equations are resolved in a Cartesian coordinate system whose origin translates at constant velocity,  $V_f$ , with the storm center of the pressure field associated with the cyclone. Variations in storm intensity and motion are represented by a series of quasi-steady state solutions. The upgraded version of the model that is applied in this study is described in (14).

The model was validated originally against winds measured in several ODGP storms. It has since been applied to nearly every recent hurricane to affect the United States offshore area, to all major storms to affect the South China Sea since 1945, and to storms affecting many other foreign basins including the Northwest Shelf of Australia, Tasman Sea of New Zealand, Bay of Bengal, Arabian Sea and Caribbean Sea. Comparisons with over-water measurements from buoys and rigs support an accuracy specification of  $\pm 20$  degrees in direction and  $\pm 2$  meters/second in wind speed (1-hour average at 10-meter elevation). Many comparisons have been published (see e.g.,15,16).

As presently formulated, the wind model is free of arbitrary calibration constants, which might link the model to a particular storm type or region. For example, differences in latitude are handled properly in the primitive equation formulation through the Coriolis parameter. The variations in structure between tropical storm types manifest themselves basically in the characteristics of the pressure field of the vortex itself and of the surrounding region. The interaction of a tropical cyclone and its environment, therefore, can be accounted for by a proper specification of the input parameters. The assignable parameters of the planetary boundary layer (PBL) formulation, namely planetary boundary layer depth and stability, and of the sea surface roughness formulation, can safely be taken from studies performed in the Gulf of Mexico, since tropical cyclones world-wide share a common set of thermodynamic and kinematic constraints. In this study the solution was compared to time histories of accurately measured surface winds from the buoys and aircraft (reduced to standard height) and as necessary the storm parameters were varied and the model iterated until good agreement was obtained between the modeled wind field and the discrete high-quality wind observations available. The resulting tropical wind field was then blended into a basin-wide field which incorporates both atmospheric modeled winds, in-situ measurements from buoys, CMAN stations, ship reports as well as satellite estimates of wind from altimeter and scatterometer instruments. Additional kinematic analysis of the tropical winds was also performed in this step including assimilation of HRD Hwind analyses as needed.

The period of Aug-25-2004 00:00 GMT to Sep-19-2004 00:00 was hindcast to allow sufficient spin-up/spin-down time for the wave and hydrodynamical models. An example of the modeled wind field is shown in Figure 2. In this study all winds are referred to the effective over-water 30-minute average winds at a height of 10 meters above sea level. The application of the following "gust" factors to the 30-minute average wind speed may derive wind speeds at shorter averaging intervals: 10-minute average x 1.09; 1-minute average x 1.24; 3-second gust x 1.53. The relative (to cyclones in other basins) richness of the in-situ wind and other meteorological data in this storm and the success of the ocean response modeling support our conclusion that the evolution of the wind field in Ivan is modeled with at least the accuracy noted above.

### Specification of the Wave Field

**Wave Model.** Oceanweather's (OWI) standard UNIWAVE high-resolution full spectral wave hindcast model was used. UNIWAVE incorporates deep water and shallow processes and the option to use either highly calibrated second generation source term physics (ODGP2) or third generation (3G) physics (OWI3G/DIA2). Recent extensive validations of these wave model variants in severe storms (17) and long-term hindcast studies (18) show excellent skill. The 3G option was selected here to provide slightly greater skill in the specification of spectral shape. Details on the 3G physics applied in UNIWAVE can be found in (19). The source term formulations are similar to those in the WAM model (20) with one important difference. When our UNIWAVE 3G variant was first tested in the early 1990s against severe GOM hurricanes including Category 5 storm Camille (1969), it was found necessary for accurate wave hindcasts to radically modify the WAM drag coefficient ( $C_{10}$ ) formulation as a function of wind speed that computes surface wind stress from 10-meter winds. Our modified drag law agrees closely with that used in WAM and gives a linear increase of  $C_{10}$  with wind speed up to wind speeds of about 25 m/s but then our  $C_{10}$  becomes asymptotic to a value of  $2.7 \times 10^{-3}$  above 30 m/s. A recent study in which  $C_{10}$  was fitted from families of GPS dropwindsonde wind profiles in the inner core of hurricanes (21) also finds that  $C_{10}$  stops increasing with wind speed above 30 m/s and may in fact decrease at greater wind speeds. UNIWAVE was applied in the GOM with grid spacing of .05 degree or 3 nm. At each point the spectrum is resolved in 24 direction bins and 23 frequency bins. The bathymetry for the model was obtained from the GEBCO (General Bathymetric Chart of the Oceans) Centenary Edition CD-ROM 1-minute dataset. The execution of the UNIWAVE hindcast model provides directly the two-dimensional wave spectrum at 15-minute intervals. Integrated properties of the spectrum are calculated from the 2-D spectrum at all northern Gulf grid points and archived as part of the hindcast run. An example of the hindcast significant wave height field in Ivan is shown in Figure 3.

**Validation.** Validation of the wave hindcast was performed against all available NDBC buoys in the Gulf of Mexico. Data were obtained from quality controlled files available from the National Oceanographic Data Center and have undergone

additional quality control procedure not possible in real-time. All wind speeds have been adjusted for height and stability to a reference level of 10 meters and all data has been smoothed +/- 1 hour with equal weighting to reduce sampling variability. CMAN stations, which do not report waves in the Gulf, were not included in the validation dataset. Time series comparisons for wind and sea state at buoys that experienced maximum impact offshore and near shore in deep water and near shore in shallow water are shown in Figures 4, 5, 6 and 7 (buoys 42001, 42003, 42040 and 42007 respectively). Similarly good skill was seen at the buoys in the far field of Ivan. Statistics for the hindcast at selected buoys are given in Table 1. The excellent time series comparisons at 42001 and 42003 imply that the hindcast depicts well the large extent of sea states offshore generated by Ivan. The good agreement west of the track at 42001 is especially encouraging because most reported 3G model hindcasts of intense hurricanes have exhibited a left-side positive bias in hindcast sea state. At 42040, the buoy directly in the path of the eye, the wind speed comparisons reveal the very large negative bias (greater than 30%) in buoy wind speed after wind speeds (adjusted in this plot to 10-meter elevation) increase above about 28 m/s. The buildup of HS to the peak of 16 m is well modeled. Note that after 0000 UTC Sep 16, the buoy data plotted have not passed the quality control because of buoy drift, and in fact since the comparison during this period are made at the nominal buoy locations the slight offset between the hindcast and measurement no doubt reflect the grid-point vs buoy location difference. At 42007, the hindcast HS is lower and the hindcast peak is slightly out of phase with the buoy. A likely explanation for these differences in such very shallow water (13 m) is that the storm surge perturbation of the water depth (not modeled) is having a significant effect on wave growth and bottom interaction. Overall all 11 buoys in the Gulf compared, the bias and scatter in modeled wind speed are -0.04 m/s and 1.27 m/s respectively. The bias and scatter for HS are -0.12 m and .49 m respectively. The bias and scatter in wave period are -.15 sec. and 2.30 seconds respectively. The relatively large scatter in period is an artifact that is a consequence of the tendency for hurricane generated spectra in the far field to be double peaked.

**Table 1** Comparison statistics for time period Sep-12-2004 to Sep-17-2004 in the Gulf of Mexico during the passage of Hurricane Ivan 2004

Station	Variable	Bias (H-M)	Std Dev	Scatter Index	Corr Coeff
42001	Ws	0.26	1.20	0.14	.96
	Wdir	-5.70	8.35	0.02	N/A
	Hs	.22	0.61	0.25	0.96
	Tave	0.44	0.61	0.27	0.87
42003	Ws	0.08	0.94	0.08	0.99
	Wdir	0.24	8.75	0.02	N/A
	Hs	0.17	0.58	0.56	0.99
	Tave	-0.51	1.12	0.14	0.95
42007	Ws	-0.11	1.86	0.19	0.96
	Wdir	0.89	8.05	0.02	N/A
	Hs	-0.51	0.57	0.33	0.98

	Tave	-0.89	2.11	0.28	0.85
42040	Ws	0.01	2.27	0.21	0.97
	Wdir	-0.30	9.51	0.03	N/A
	Hs	-0.45	0.46	0.15	0.99
	Tave	-0.12	1.39	0.18	0.93

### Specification of Ocean Currents

**Model.** The simulation of currents used the Hybrid Coordinate Ocean Model – HYCOM (13). A multi-institutional effort, funded by the US National Ocean Partnership Program (NOPP), is developing and evaluating this data-assimilative hybrid isopycnal-sigma-pressure (generalized) co-ordinate ocean model – HYCOM (for more details, see <http://oceanmodeling.rsmas.miami.edu/hycom/>)

In addition to the standard model set-up from the HYCOM Consortium, the version used here benefits from some additional features added by the Nansen Environmental and Remote Sensing Center (NERSC). These include the capability of coupling with other models, such as a biological model and a dynamic-thermodynamic ice model and a flexible data assimilation framework (22). In addition, improvements to the numerical solution of the momentum and advection equations have been implemented, which includes the use of higher order schemes with better capabilities for resolving small-scale features, such as eddies. The upper layers are better resolved with the upper most layer just 3 m thick as opposed to 10 m thickness in the previous version thereby allowing improved specification of surface currents. The bathymetry was specified using the GEBCO (same source as used for the wave model). This study was undertaken by nesting a fine resolution HYCOM model grid, covering the Gulf of Mexico, into the coarser resolution TOPAZ model system. The TOPAZ model grid covers the Arctic Ocean and the Atlantic Ocean to approximately 60° south. The model grid and bathymetry are shown in Figure 8. The nested model grid used for the Gulf of Mexico has a resolution of approximately 5km. Both models were run with 22 hybrid layers in the vertical.

**Validation.** Unfortunately, no public domain measurements of currents are available during the passage of Hurricane Ivan in the GOM. The model has been validated against data in a previous storm, Hurricane Andrew, 1992, in which significant measured data sets exist, namely the current meter data set collected during the Minerals Management Service's LATEX project (see <http://www-ocean.tamu.edu/Quarterdeck/QD4.2/latex-4.2.html#anchor700340>) and for which high-quality atmospheric forcing was available from the previous MMS Andrew program. The only drawback to using Hurricane Andrew for validation of the HYCOM model is that it occurred in August 1992, which is before satellite altimetry data were available. Such data are normally assimilated into HYCOM to help describe the actual dynamics of the Gulf of Mexico (position of eddies, of the Loop Current etc.) during the period being modeled. The Andrew simulation was

therefore, initialized with an arbitrary model state, spun up for four months with atmospheric fields from 1992. Boundary conditions were calculated from the basin scale outer model, which was run for the same time period in 1992. The Andrew model validation is described in more detail in (3).

**Initialization.** An improved climatology (GDEM3, previously Levitus) has been used to initialize the model. This improved the stratification in the intermediate and deep waters of the Gulf. The stratification of the ocean is an important property, in terms of current response to the passage of a hurricane. In the Gulf of Mexico, warm-core eddies often shed off the Loop Current and drift westwards into the western Gulf of Mexico. The interior of eddies and of the Loop Current is a very different oceanographic regime from that of the resident Gulf waters. The anticyclonic eddies are associated with a deep and warm mixed layer at their centers. The presence of an eddy can influence such effects as inertial oscillations after the passage of the hurricane, as well as the depth of the mixed layer due to mechanical stirring. The model was spun up from the year 2002 until the Ivan study period. Figure 9 compares the model and satellite sea surface anomalies in the Gulf of Mexico after spin up. It is clear that even without satellite data assimilation the initial state is reasonably similar to the satellite altimetry map in the area of study, with one warm eddy located to the north of the Loop Current.

**Model Run and Forcing.** During the actual passage of Hurricane Ivan, high-frequency wind fields (given every 15 min and with a resolution of  $0.05^\circ$ ) provided by Oceanweather were used. The model was integrated from the 8<sup>th</sup> to the 22<sup>nd</sup> of September 2004 with high frequency wind forcing from Oceanweather from 7<sup>th</sup> to the 19<sup>th</sup> of September.

**Model Output.** Time series of full model profiles were provided north of 26N and west of 96W at every grid cell. In addition an animation of the instantaneous surface current velocity state every 6 hours was generated. Figure 10 shows a snapshot of the surface currents. The model results show the extremely strong surface currents associated with the passage of the hurricane and the inertial wake on the days after the passage.

## Results and Conclusions

The temporal and spatial evolution of surface winds, sea state and currents in the northern GOM in Hurricane Ivan is resolved by the application of advanced numerical ocean response models driven by wind and pressure fields carefully developed using all available meteorological data. The intensive real time monitoring of Ivan combined with a relatively rich base of in-situ, aircraft and satellite meteorological data have allowed us to derive an accurate specification of the forcing required by the response models. The measured data allowed a comprehensive validation of the wave hindcast. It was shown that the proven OWI hurricane wind and wave hindcasting technology well simulated the sea states excited by Ivan both in the intense inner core of the storm and the peripheral region. The bias in significant wave height and period are of order 10 cm and 0.5 s respectively and the correlation between measurements and model is 0.95

or better at measurements sites in deep and shallow water.

The question of how a Category 3 storm could excite peak sea states heretofore thought to be associated with more intense hurricanes is answered implicitly by the success of the hindcast. Simply, the particular combination of Ivan's intensity history (it was after all a Category 5 storm when it entered the Gulf), its several cycles of eyewall replacement which led at times to a large radius of maximum wind, its evidently optimum forward velocity for ocean response and its large outer core wind field structure all conspired to allow Ivan to generate record (measured) peak sea states for a Gulf hurricane (HS of about 16 m) in its right front quadrant.

In the case of the ocean circulation model hindcast, since no in-situ current data were available in the northern Gulf during Hurricane Ivan, it is not possible to make any direct assessment of the quality of the Ivan current hindcast data. The previous hindcast and validation of hurricane Andrew suggests that current hindcasts, especially of current direction, are more biased and scattered than wave hindcasts but that, at least for the primary response, peak near surface current speeds may be specified near the track with bias of the order of +25 cm/s albeit with considerable scatter.

The hindcast reported here has produced a digital data base of the hindcast time series of wind, wave, salinity, sea surface temperature and current results for all active grid points north of 26N and west of 96 W in the GOM. This database allows ready interpolation of storm peaks at any specific site of interest. For example, Table 2 lists the peak hindcast winds, sea states and currents (multiple depths) at 29 N 88 W, which is located in deep water just southeast of buoy 42040. Results such as these are critical to engineering investigations of the impact of Ivan at specific platform locations and along specific pipeline routes.

**Table 2 Peak hindcast values at grid 29.0N 88.0W**

Wave Grid Point	57368
Latitude	29.0000
Longitude	-88.0000
Depth(m)	1321.00
CYM of Peak Wave	200409
DHM of Peak Wave	152215
Maximum Wind Speed (30 min m/s)	46.8
Assoc Wind Direction (met. deg)	104.0
Sig. Wave Ht (m)	16.1
Sig. Wave Period (s)	11.7
Wave Direction (ocean. deg)	315.3
Maximum Wave (m)	27.8
Crest Height (m)	15.6

Max Current Speed at 5m (cm/s)	251
Assoc Current Direction at 5m (ocean. deg)	319
Assoc Current Speed at 75m (cm/s)	72
Assoc Current Direction at 75m (ocean. deg)	337
Assoc Current Speed at 150m (cm/s)	18
Assoc Current Direction at 150m (ocean. deg)	197
Assoc Current Speed at 700m (cm/s)	11
Assoc Current Direction at 700m (ocean. deg)	219

## References

- Cardone, V.J., A.T.Cox, J.A. Greenwood, D.J. Evans, H Feldman, S.M. Glenn, T. R. Keen. Hindcast Study of Winds, Waves and Currents in Hurricane Andrew, Gulf of Mexico, 1994: Final Report to Minerals Management Service, Herndon, VA.
- Puskar, F. J., R. K. Aggarwal, C.A. Cornell, F. Moses, C. Petrauskas, 1994. A Comparison of Analytically Predicted Platform Damage to Actual Platform Damage During Hurricane Andrew. 26<sup>th</sup> Annual Offshore Technology Conference, Houston. Paper No. OTC 7473.
- Cardone, V. J, A. T. Cox, K. A. Lisaeter and D. Szabo, 2004. Hindcasts of Winds, Waves and Currents in Northern Gulf of Mexico in Hurricane Lili (2002). Offshore Technology Conference, Houston. Paper OTC 16821.
- Ward, E. G., 1974. Ocean Data Gathering Program – An Overview. Seventh Annual Offshore Technology Conference, Houston, TX. Paper No. OTC 2332.
- Sanford, T.B., P.G. Black, J.R. Hausteijn, J.W. Feeney, G. Z. Forristall, and J. F. Price, 1987. Ocean Response to a Hurricane, *J. Phys. Oceanogr.*, 17,2065-2083.
- Petrauskas, C., T. D. Finnegan, J. C. Heideman, M. Vogel, M. Santala and G. P. Berek, 1994. Metocean Criteria/Loads for Use in Assessment of Existing Offshore Platforms. 26<sup>th</sup> Offshore Technology Conference, Houston. Paper No. OTC 7484.
- Cardone, V. J. and R. Ramos, 1998. Wave, Wind and Current Characteristics of Bay of Campeche. 30<sup>th</sup> Offshore Technology Conference, Houston, TX. Paper No. OTC 8697.
- Cardone, V. J., W. J. Pierson and E. G. Ward. 1976. Hindcasting the directional spectra of hurricane generated waves. *J. of Petrol. Technol.*, 28, 385-394.
- Ward, E. G., L. E. Bogman and V. J. Cardone, 1979. Statistics of Hurricane Waves in the Gulf of Mexico. *J. of Petrol. Technol.*, 31, 632-642.
- Haring, R. E. and J. Heideman, 1979. Gulf of Mexico Rare Wave Return Periods. 10<sup>th</sup> Annual Offshore Technology Conference, Houston, TX. Paper No. OTC 3229.
- Forristall, G. Z., 1980. A Two-Layer Model for Hurricane Driven Currents on an Irregular Grid, *J. Phys. Oceanogr.*, 10, 1417-1438.
- Reece, A. M. and V. J. Cardone, 1982. Test of Wave Hindcast Model Results against Measurements during Four Different Meteorological Systems, Offshore Technology Conference, Houston, TX, Paper No. OTC 4323.
- Bleck, R., 2002: An Oceanic General Circulation Model framed in Hybrid Isopycnic-Cartesian Coordinates, *Ocean Modelling*, 4, 55-88, 2002
- Thompson, E. F. and V. J. Cardone. 1996. Practical modeling of hurricane surface wind fields. *ASCE J. of Waterway, Port, Coastal and Ocean Engineering*. 122, 4, 195-205.
- Forristall, G. Z., E. G. Ward, V. J. Cardone, and L. E. Borgman. 1978. The Directional Spectra and Kinematics of Surface Waves in Tropical Storm Delia. *J. of Phys. Oceanog.*, 8, 888-909.
- Cardone, V. J. and D. T. Resio, 1998. An Assessment of Wave Modeling Technology. Preprints of 5<sup>th</sup> International Workshop on Wave Hindcasting and Forecasting. Melbourne, Fl. January 26-30, 1998.
- Cardone, V. J., R. E. Jensen, D. T. Resio, V. R. Swail and A. T. Cox. 1996. Evaluation of Contemporary Ocean Wave Models in Rare Extreme Events: Halloween storm of October, 1991; Storm of the century of March, 1993. *J. of Atmos. and Ocean. Tech.*, 13, 198-230.
- Cox, A.T. and V.R. Swail. A Global Wave Hindcast over the Period 1958-1997: Validation and Climate Assessment. *JGR (Oceans)*, Vol. 106, No. C2, pp. 2313-2329, February 2001.
- Khandekar, M. L., R. Lalbeharry and V. J. Cardone. 1994. The Performance of the Canadian Spectral Ocean Wave Model (CSOWM) during the Grand Banks ERS-1 SAR Wave Spectra Validation Experiment. *Atmosphere-Oceans*, 32, 31-60.
- WAMDI Group, 1988. The WAM model - a Third Generation Ocean Wave Prediction Model. *J. Phys. Ocean.* 18: 1775-1810.
- Powell, M.D., P.J. Vickery and T. A. Reinhold, 2003. Reduced Drag Coefficient for High Wind Speeds in Tropical Cyclones. *Nature*, 422, 279-283.
- Brusdal, K., J. Brankart, G. Halberstadt, G. Evensen, P. Brasseur, P. J. van Leeuwen, E. Dombrowsky, and J. Verron, *An evaluation of ensemble based assimilation methods with a layered OGCM*, *J. Marine. Sys.*, 40-41, 253-289, 2003.

Table

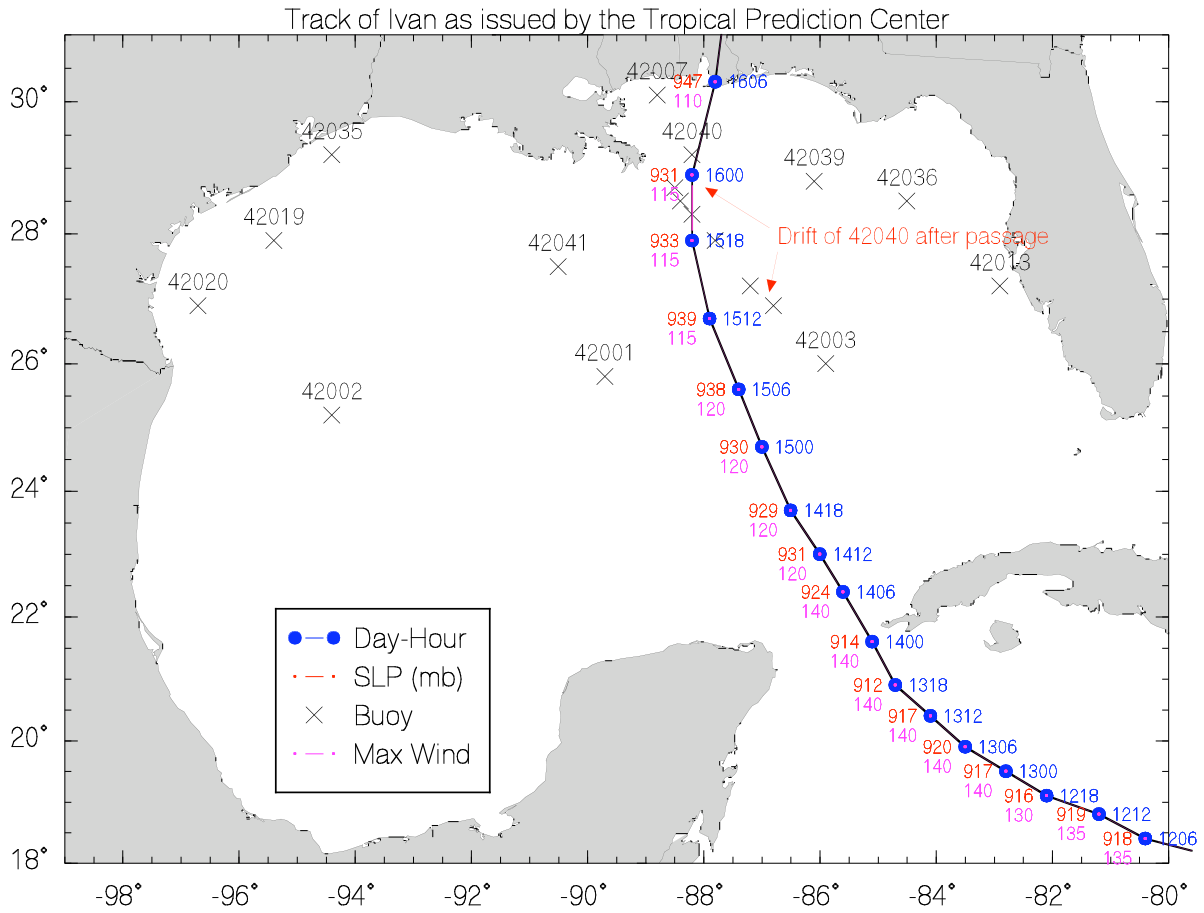


Figure 1 Track of Ivan in Northern Gulf of Mexico with fix time (circle right, GMT, DDHMM), central pressure (circle left, mb) and NDBC buoy locations ('X's).

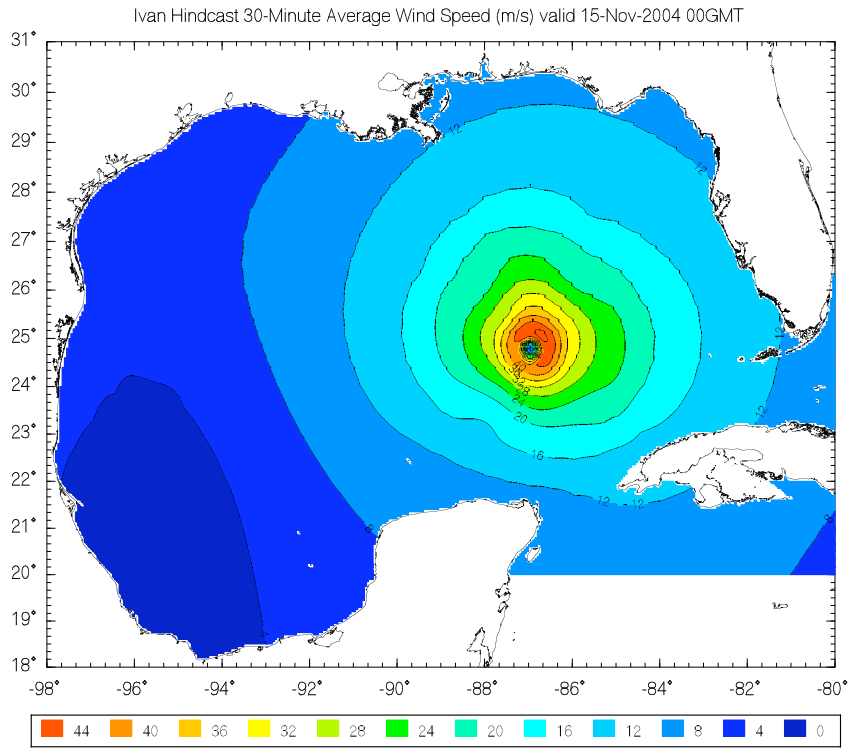


Figure 2 Typical hindcast wind speed (m/s) during Hurricane Ivan 2004

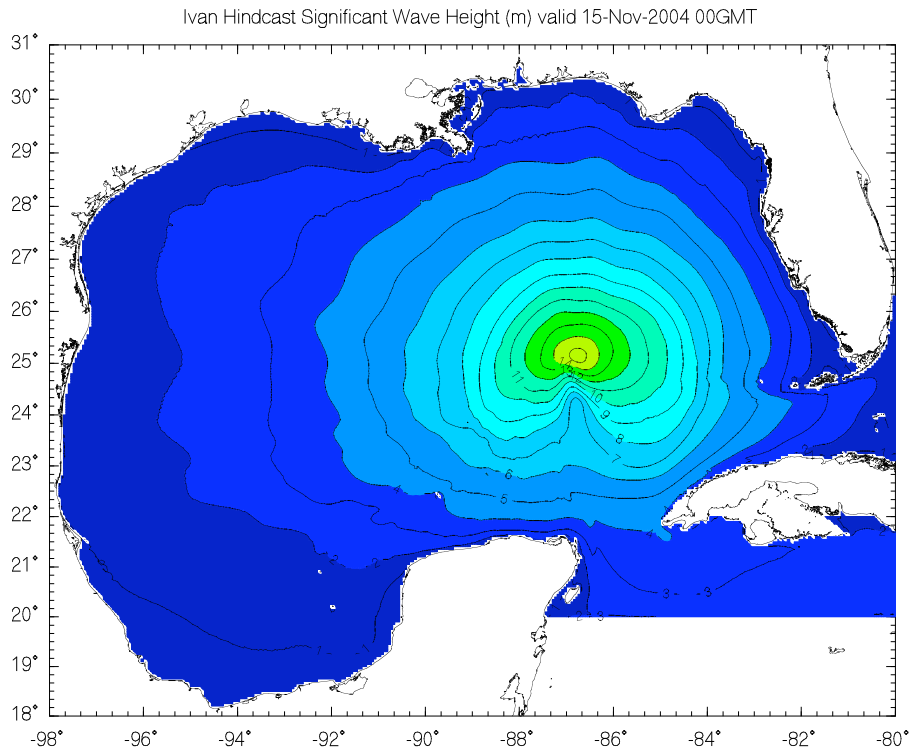
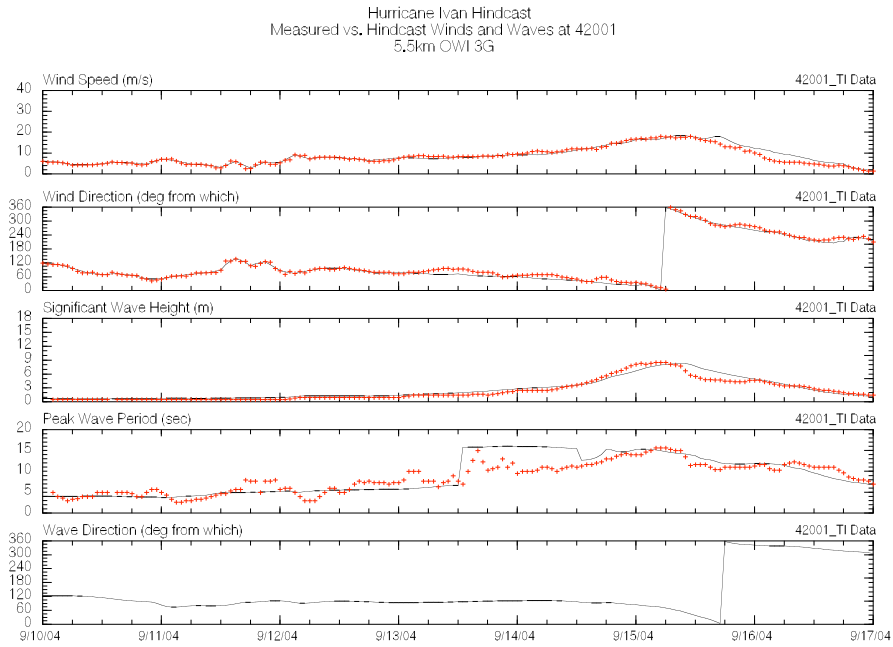
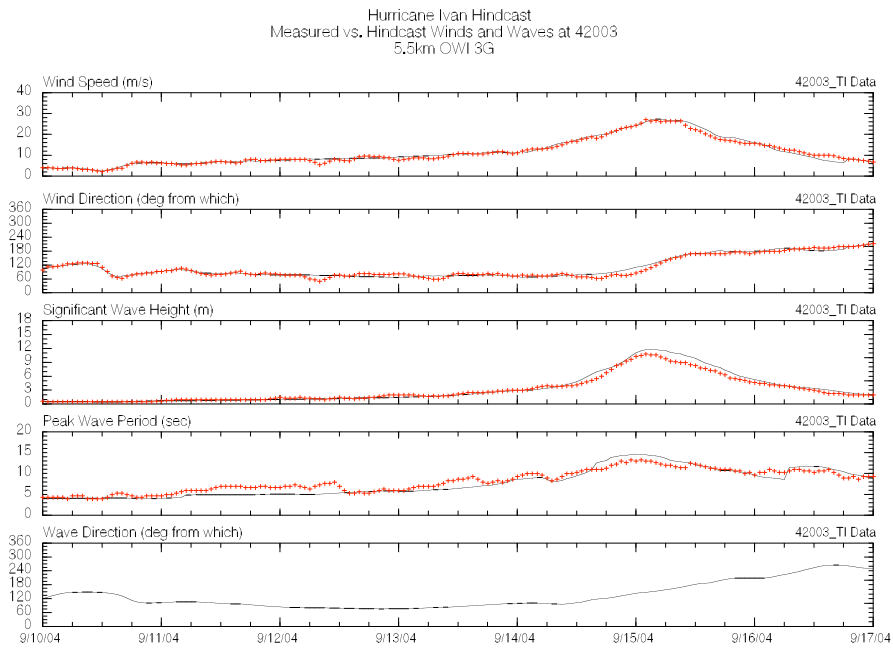


Figure 3 Typical hindcast significant wave height (m) hindcast during Hurricane Ivan 2004



**Figure 4 Timeseries comparison of wind speed (m/s), wind direction (met deg), significant wave height (m), average wave period (s) and wave direction (met deg) at NOAA buoy 42001 during Hurricane Ivan 2004**



**Figure 5 Timeseries comparison of wind speed (m/s), wind direction (met deg), significant wave height (m), average wave period (s) and wave direction (met deg) at NOAA buoy 42003 during Hurricane Ivan 2004**

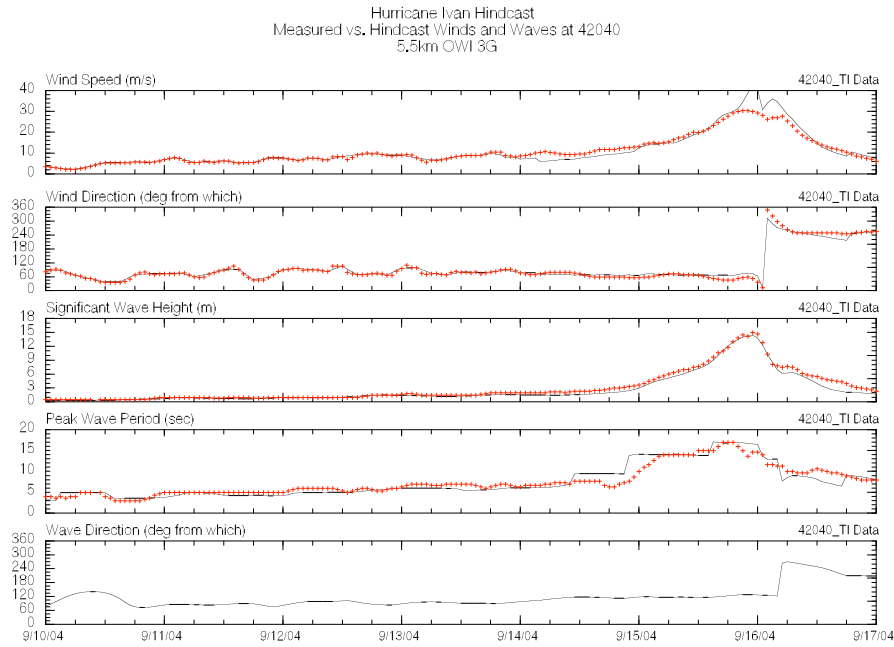


**Figure 6** Timeseries comparison of wind speed (m/s), wind direction (met deg), significant wave height (m), average wave period (s) and wave direction (met deg) at NOAA buoy 42040 during Hurricane Ivan 2004

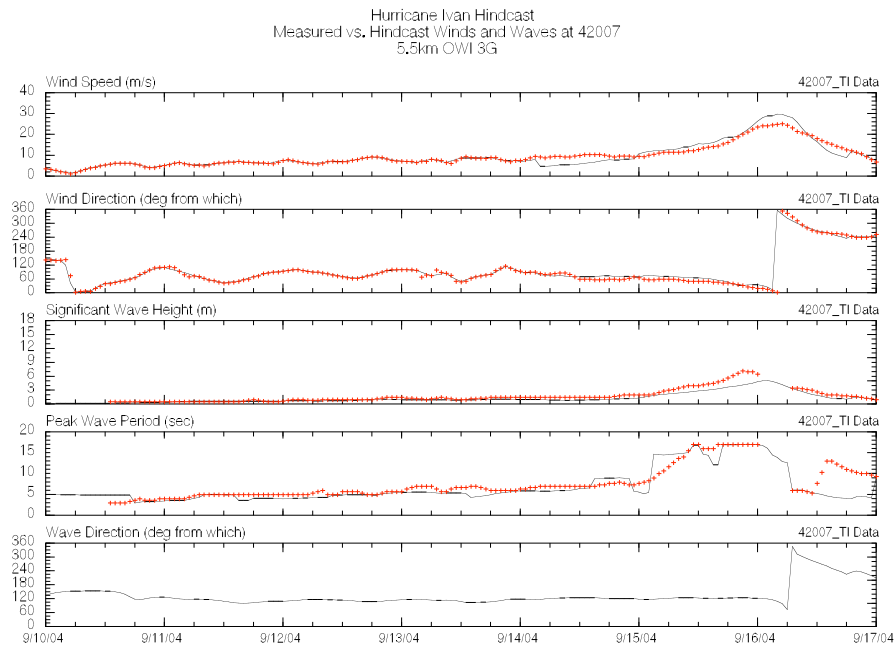


**Figure 7** Timeseries comparison of wind speed (m/s), wind direction (met deg), significant wave height (m), average wave period (s) and wave direction (met deg) at NOAA buoy 42007 during Hurricane Ivan 2004

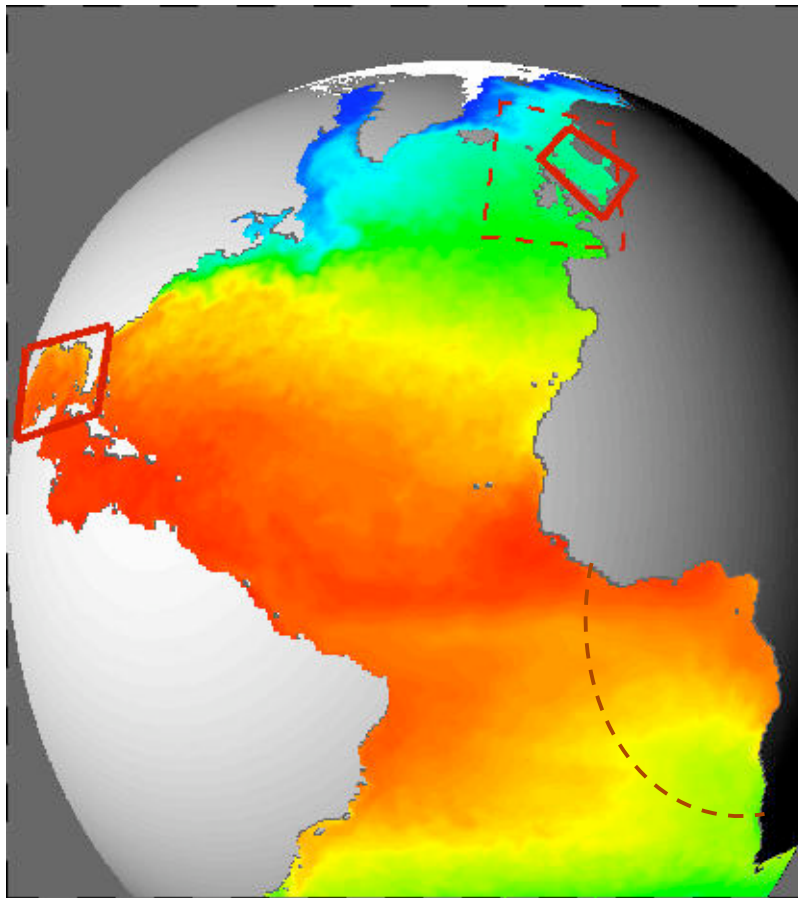


**Figure 8** The TOPAZ model system with nested models. The solid lines indicate high-resolution regional models already running in real-time and the dashed lines indicate those presently being developed at NERSC. Sea surface temperatures are shown here. Full forecast bulletins are updated on <http://topaz.nersc.no>

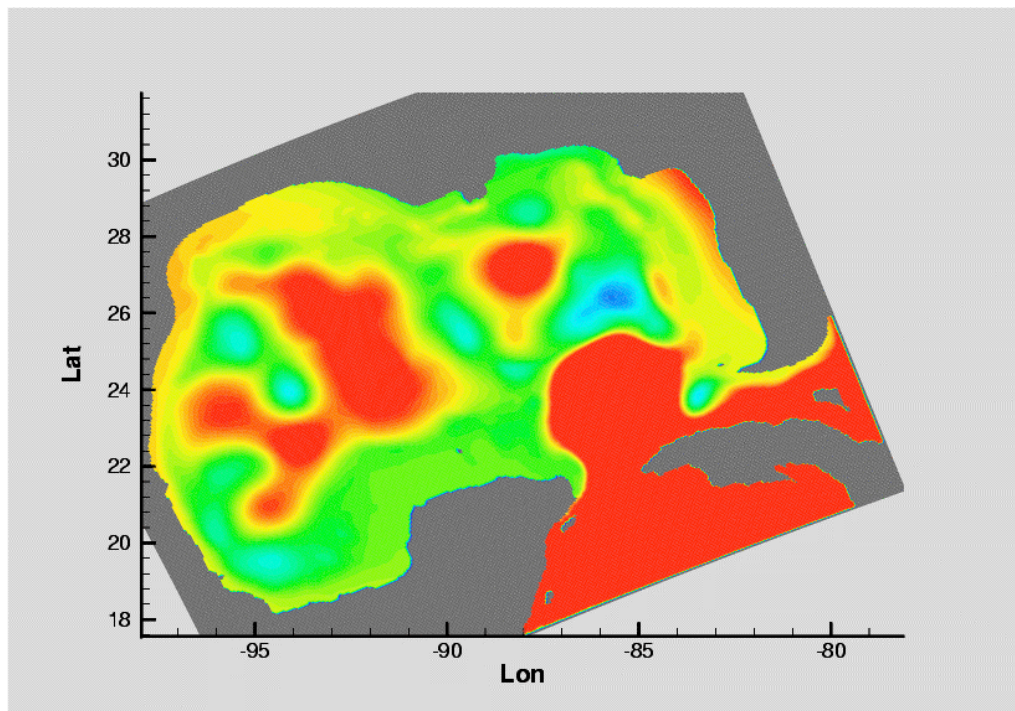


Figure 9a Model SSH on the 8<sup>th</sup> of September

SSALTO/DUACS – NRT SSH – Merged product  
8-Sep-2004 (CNES day 19974)

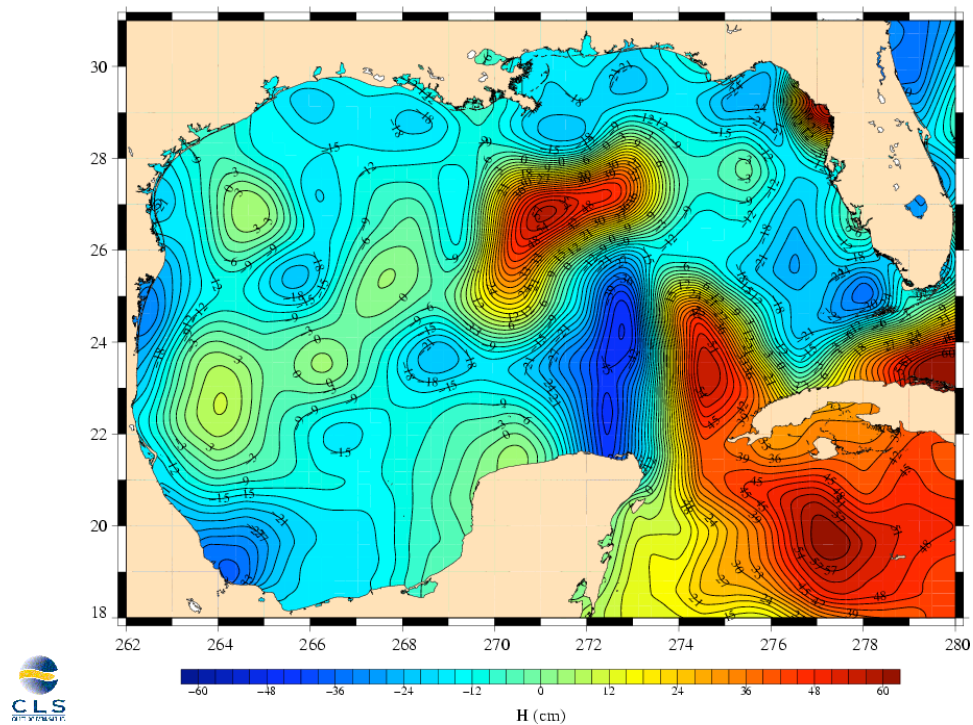
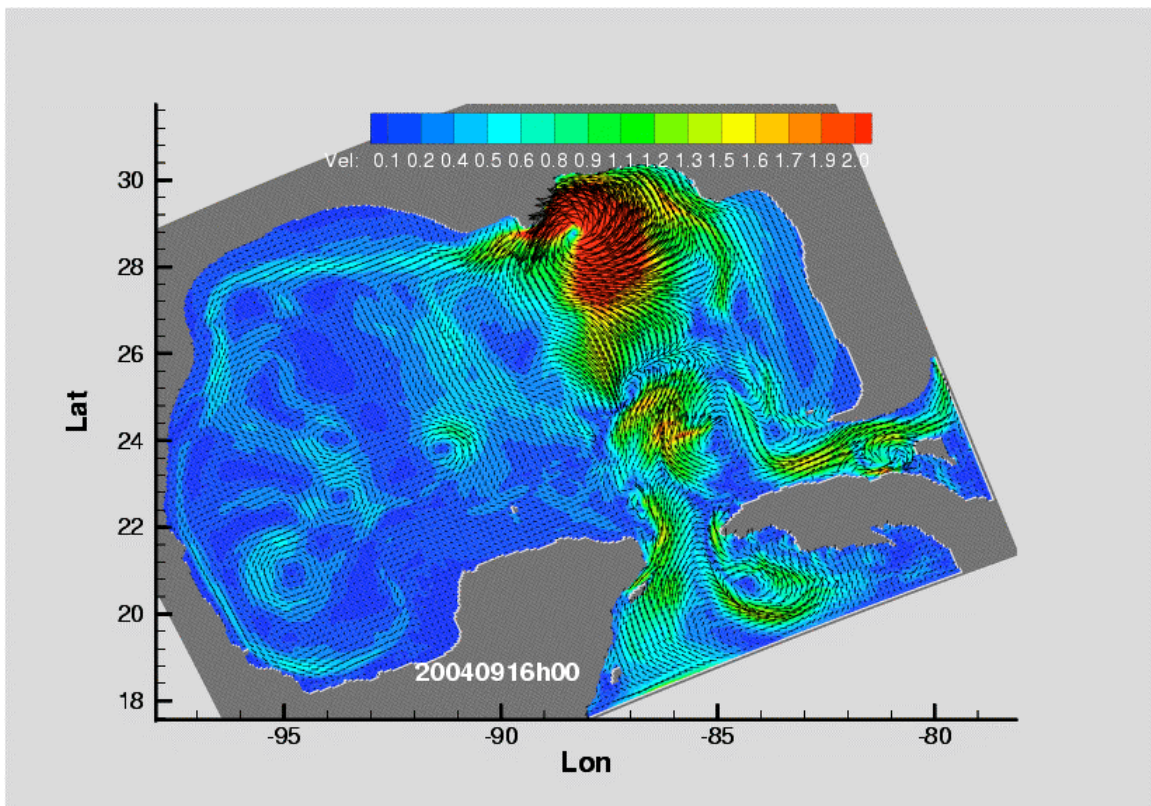


Figure 9b CLS remote sensing chart of SSH On the 8<sup>th</sup> of September



**Figure 10** Model instantaneous surface current velocity on the 16<sup>th</sup> of September, midnight